Protein Thiol Oxidation in Murine Airway Epithelial Cells in Response to Naphthalene or Diethyl Maleate

Page C. Spiess[1], Dexter Morin[1], Chase R. Williams[1], and Alan R. Buckpitt[1]

[1]Department of Molecular Biosciences, School of Veterinary Medicine, University of California, Davis, Davis, California

Naphthalene (NA) is a semivolatile aromatic hydrocarbon to which humans are exposed from a variety of sources. NA results in acute cytotoxicity to respiratory epithelium in rodents. Cytochrome P450-dependent metabolic activation to form reactive intermediates and loss of soluble cellular thiols (glutathione) are critical steps in NA toxicity, but the precise mechanisms by which this chemical results in cellular injury remain unclear. Protein thiols are likely targets of reactive NA metabolites. Loss of these, through adduction or thiol oxidation mechanisms, may be important underlying mechanisms for NA toxicity. To address the hypothesis that loss of thiols on specific cellular proteins is critical to NA-induced cytotoxicity, we compared reduced to oxidized thiol ratios in airway epithelial cell proteins isolated from lungs of mice treated with NA or the nontoxic glutathione depletor, diethyl maleate (DEM). At 300 mg/kg doses, NA administration resulted in a greater than 85% loss of glutathione levels in the airway epithelium, which is similar to the loss observed after DEM treatment. Using differential fluorescent maleimide labeling followed by 2DE separation of proteins, we identified more than 35 unique proteins that have treatment-specific differential sulfhydryl oxidation. At doses of NA and DEM that produce similar levels of glutathione depletion, Cy3/Cy5 labeling ratios were statistically different for 16 nonredundant proteins in airway epithelium. Proteins identified include a zinc finger protein, several aldehyde dehydrogenase variants, β-actin, and several other structural proteins. These studies show distinct patterns of protein thiol alterations with the noncytotoxic DEM and the cytotoxic NA.

Keywords: thiol oxidation; bronchial epithelial cells; naphthalene; diethyl maleate; proteomics

CLINICAL RELEVANCE

These studies compare the post-translational modification of protein thiols in airway epithelial cells in response to exposure to the glutathione depletors, naphthalene, a Clara cell–selective cytotoxic agent and diethyl maleate which is not toxic. Enhanced understanding of the biochemical mechanisms for chemical-induced lung toxicity associated with airborne toxics, like naphthalene, will aid in predicting sensitive populations and in devising ways to ameliorate the health consequences of exposure.

Naphthalene (NA) is a well-studied environmental pollutant that, in mouse models, selectively results in necrotic lesions of nonciliated bronchiolar epithelial cells (Clara cells) regardless of route of exposure (oral, intraperitoneal, or inhalation) (1, 2). Similar toxicity is not observed in rat lung, which raises the issue of potential susceptibility of the respiratory tract of humans. Widespread exposure of humans to NA has been documented. NA is a byproduct of combustion of wood and gasoline (3) and is a significant component of jet fuel (1–3%). High concentrations of NA and structural congeners are found in mainstream and side-stream tobacco smoke (4). As demonstrated recently, food may be a source of human exposure as well (5). The Centers for Disease Control and Prevention's National Health and Nutrition Examination Survey conducted a study in 2001 and 2002 of 2,748 United States citizens to determine their exposure to polycyclic aromatic hydrocarbons (PAHs). NA metabolites were detected in 100% of the population examined, and, of the 22 hydroxy-PAH metabolites measured, naphthols accounted for 75% of the total PAHs detected (6). Epidemiologic studies have failed to establish a link between NA exposure and lung disease, although this may be due to the high incidence of lung disease and to the prevalence of human exposure to this compound. Thus, proper assessment of the susceptibility of human populations depends on understanding key steps associated with the mechanisms of toxicity in animal models, the development of biomarkers that probe these key steps, and by application of these to exposed human populations.

NA is metabolized by cytochrome P450s into highly reactive electrophilic intermediates, some of which can be detoxified by conjugation with glutathione (GSH). Depletion of GSH is a major determinant in NA respiratory toxicity; depleting GSH increases adduct formation and enhances susceptibility to NA toxicity (7, 8). Similarly, augmenting GSH levels with GSH monoethylester or cysteinyl-glycine decreases toxicity and covalent binding of reactive NA metabolites (9). Further studies also have shown that diethyl maleate (DEM), a GSH depletor, causes significant GSH loss in intrapulmonary airways that is quantitatively similar to NA but does not result in the same cellular cytotoxicity as that caused by NA exposure (e.g., increased membrane permeability, mitochondrial disruption, and cell death) (9). Thus, GSH depletion is a necessary but not sufficient feature of NA-induced airway epithelial cell injury.

Reactive NA intermediates can covalently adduct proteins, and there is a general association between the levels of adducted protein in the lung and the severity of airway epithelial cell toxicity (10). More recent studies have identified a number of proteins within airway epithelial cells that are adducted by reactive NA metabolites, but the specific metabolites involved in adduct formation and the role of quinone redox cycling compared with covalent adduct formation in cytotoxicity remains unclear (11–14). Many of the adducted proteins identified are involved in protein folding and maintenance of proper cellular redox status, leading to the possibility that the mechanism of toxicity may be a combination of adduction of critical proteins and the oxidation of cellular protein thiols associated with redox cycling. Protein thiol oxidation is also a possible result of NA metabolism, either because of GSH depletion or direct oxidation caused by reactive oxygen species formed during redox cycling of NA

(*Received in original form April 21, 2009 and in final form August 17, 2009*)

This work was supported by NIEHS grants 04311 and 04699 by an NIEHS predoctoral training fellowship (ES007059–30) (P.C.S.).

Correspondence and requests for reprints should be addressed to Page C. Spiess, Ph.D., Department of Pathology, University of Vermont, 89 Beaumont Ave., Given C264, Burlington, VT 05405. E-mail: pspiess@uvm.edu

Am J Respir Cell Mol Biol Vol 43. pp 316–325, 2010
Originally Published in Press as DOI: 10.1165/rcmb.2009-0135OC on October 20, 2009
Internet address: www.atsjournals.org

metabolites. A recent study by Dennehy and colleagues (15) indicated that modification of specific protein families was possible by thiol-reactive electrophiles. Thus, understanding changes in the redox status of cellular proteins may yield significant insight into mechanisms by which chemicals can produce cellular necrosis.

We have recently reported a method that allows measurement of the ratio of reduced to oxidized cellular protein thiols using differential fluorescence labeling combined with gel electrophoresis (16). The current study uses this method to address the differences in protein thiol oxidation caused by NA and DEM in airway epithelial cells of male mice after intraperitoneal administration. We identified specific proteins in which thiols were oxidized by NA and were not oxidized by DEM or were differentially oxidized by DEM relative to control protein samples. Specific doses of these chemicals produced equivalent GSH loss in the liver and in airway epithelial cells. Comparisons of protein thiol loss associated with the cytotoxic aromatic hydrocarbon NA with the noncytotoxic GSH depletor DEM focus attention on target proteins possibly involved in the series of events leading to the cytotoxic injury associated with NA.

MATERIALS AND METHODS

The method used in the current work is the same as in a recently published paper describing the procedures for monitoring protein thiol status using differential fluorescence labeling coupled with protein separation by two-dimensional (2D) gel electrophoresis (16). Therefore, abbreviated descriptions are provided here.

Reagents

NA was purchased from Fisher Scientific (Pittsburgh, PA), and DEM was purchased from Sigma-Aldrich, Inc. (St. Louis, MO). Nondetergent sulfobetaine-195, benzamidine, 1,10-phenanthroline, aprotinin, pepstatin, and leupeptin were obtained from Calbiochem (La Jolla, CA). Rhinohide acrylamide/bisacrylamide was obtained from Molecular Probes (Eugene, OR). Bio-Rad Protein Assay solution was purchased from Bio-Rad (Hercules, CA). Sea Plaque low-melting-temperature agarose and Isogel agarose were obtained from Cambrex BioScience Rockland, Inc. (Rockland, ME). Cy3 and Cy5 maleimide monoreactive dyes and all other electrophoresis materials were obtained from GE Health Care (Piscataway, NJ). These dyes are not the CyDIGE maleimides; rather, they are disulfonic acid maleimides. All solutions were prepared with deionized water (resistivity $\geq$ 18.1 MΩ/cm).

Animals and Treatment

All animal use was approved by the Animal Use and Care Committee at the University of California, Davis. Male Swiss Webster ND4 mice (25–30 g) were purchased from Harlan (Indianapolis, IN). Animals were allowed free access to food and water and were housed in an Association for Assessment and Accreditation of Laboratory Animal Care–accredited facility in HEPA-filtered cage racks at the University of California, Davis, for at least 5 days before use. Twenty-four mice were randomly assigned to one of four treatment groups (n = 6 per group): 200 mg/kg NA, 300 mg/kg NA, 1 g/kg DEM, or oleic oil vehicle control. For all experiments, animals were given a single intraperitoneal dose of NA, DEM, or a corresponding volume of oleic oil vehicle control (0.05 ml/10 g body weight). Animals were killed 1 hour after DEM or oleic oil injection or 2 hours after NA injection with an overdose of pentobarbital.

Recovery of Epithelial Cell Proteins by Lysis-Lavage

Procedures for selective removal of airway epithelial cell proteins were described by Wheelock and colleagues (17). Briefly, the trachea of each animal was cannulated, the parenchymal portions of this organ were protected by infusion of low-melting-temperature agarose followed by 5% dextrose, and the excised lung was cooled in ice-cold 5% dextrose. After 10 minutes, the dextrose solution was removed through simultaneous inversion of the lungs and gentle suction with a syringe; this procedure was repeated until no more solution could be recovered. The airways were then lavaged with lysis buffer containing detergents, protein denaturants, and protease inhibitor cocktail as described (16) to recover airway epithelial proteins. The residual lung, a small liver sample, and 50 μl of lysis lavage sample from each animal were homogenized in Solution A (200 mM methane sulfonic acid, 5 mM diethylenepentaacetic acid) for GSH analysis. Samples were frozen immediately on dry ice.

GSH Analysis by HPLC

A method previously described by Lakritz and colleagues (18) was used for the quantification of GSH. Briefly, the supernatant from centrifuged acidic lysis lavage, residual lung, and liver samples was subjected to reverse-phase HPLC coupled with electrochemical detection to directly measure reduced GSH. The response was linear from 0.25 to 1,000 ng of GSH on column (r^2 = 0.996), and data are reported as nmol of GSH per mg protein, as determined by the Bradford protein assay (19). Statistical comparisons of GSH levels between groups were made using a one-way ANOVA in SigmaStat 3.0. Differences were considered significant at $P \leq 0.05$.

Multiplexed Fluorescent Labeling and 2DE

This method was first described by Spiess and colleagues (16). Each lavage sample, containing approximately 1 mg protein, was added immediately to tubes containing 250 nmol Cy3 maleimide dye for labeling of reduced thiols within the sample. Cy3 maleimide–labeled samples were incubated at room temperature in the dark overnight (for at least 16 h), which allowed excess unreacted dye adequate time to hydrolyze within the aqueous lysis solution. Tributylphosphine (40 μl of 200 mM stock) was added to each sample (24 mM final concentration) and allowed to incubate for 30 minutes to reduce disulfide bonds and sulfenic acids. Each sample was then reacted with 250 nmol of Cy5 maleimide by incubating at room temperature for at least 2 hours.

Samples from individual animals were analyzed independently. Immobilized pH gradient (IPG) buffer was added to 100 μg of protein from each sample, and sample volumes were brought to 350 μl with lysis solution. Two narrow-range, 18-cm Immobiline DryStrips (GE Health Care, Piscataway, NJ) (pH 4.5–5.5 and pH 5.5–6.7) were rehydrated for each sample. Protein separation by 2D gel electrophoresis was performed as described previously (16). After electrophoresis, the protein gels were fixed in 25% methanol, 5% acetic acid overnight.

Visualization of Labeled Proteins

All gels were scanned for Cy3 and Cy5 signal using a Typhoon 8600 at 100 μm resolution. Photomultiplier settings varied between 400 and 800 mV and were set to the highest levels possible without signal saturation. Gels were silver stained as described (16) to register features for identification. Silver-stained gels were scanned at a resolution of 600 dpi on an Epson Expression 1680 flatbed scanner (Epson American, Long Beach, CA) (16 bit grayscale) using the SilverFast EpsonIT8 software. Gels were warped to align spots using TT900 S2S v2006, and spot volume analysis of the gels was performed in Progenesis PG220 v2006 (both Nonlinear Dynamics, Durham, NC). Elementary spot volume calculations were performed in Microsoft Excel.

Statistical Analysis

A Cy3/Cy5 spot volume ratio was calculated for each spot. Statistical comparisons of spot volumes between groups were made using a one-way ANOVA in SigmaStat 3.0. Differences were considered significant at $P \leq 0.05$.

Protein Identification by Matrix Assisted Laser Desorption/Ionization Tandem Time-of-Flight Mass Spectrometry and Liquid Chromatography-Tandem Mass Spectrometry

Proteins whose Cy3/Cy5 ratios were identified as being significantly different between treatment groups were excised from the control 2D gels. Gel plugs were destained, washed, and digested with trypsin

(modified trypsin gold [10 ng/μl]; Promega, Madison, WI). Analysis of peptides was performed on an Applied Biosystems 4700 Proteomics Analyzer (Applied Biosystems Inc., Foster City, CA) with Tandem Time-of-Flight (TOF/TOF) optics. Matrix Assisted Laser Desorption/Ionization–Mass Spectrometry (MALDI-MS) data were collected in the m/z range of 700 to 4000 using trypsin autolysis peaks of m/z 842.510, 1,045.600, 2,211.105, and 2,239.136 Da as internal calibrants. Data were analyzed using Applied Biosystems GPS Explorer Software with a precursor tolerance of 100 ppm, MS/MS fragment tolerance 0.2 Da, and the following variable modifications: oxidation (M), Cy3 (C), Cy5 (C), and a maximum of two missed trypsin cleavages. The IPI Mouse database searches (53,847 entries) were performed on all MS and MS/MS data sets using GPS Explorer Workstation v3.5 software (Applied Biosystems, Inc., Foster City, CA), and a probability-based Mascot score greater than 60 (equivalent to $P \leq 0.05$) was considered a statistically significant hit.

Digested tryptic peptide samples that could not be identified by MALDI-TOF/TOF were analyzed by Liquid Chromatography-Tandem Mass Spectrometry (LC-MS/MS) at the University of California, Davis Proteomics Facility. Peptides were directly loaded onto an Agilent ZORBAX 300SB C_{18} reverse phase trap cartridge (Santa Clara, CA), which, after loading, was switched in-line with a Michrom Magic C_{18} AQ 200 μm × 150 mm C_{18} column (Auburn, CA) connected to a Thermo-Finnigan LTQ iontrap mass spectrometer (San Jose, CA) through a Michrom Advance Plug and Play nano-spray source. Peptides were separated using a gradient of 2 to 40% B (A = 0.1% formic acid; B = 100% ACN) over 35 minutes, a gradient of 40 to 80% B for 1 minute, held for 1 minute, and a gradient of 80 to 2% B over 8 minutes. MS and MS/MS spectra were acquired using a top 10 method, where the top 10 ions in the MS scan were subjected to automated low-energy CID. All MS/MS samples were analyzed using Mascot. Mascot was set to search the NCBI mouse database (140,245 entries), assuming the digestion enzyme trypsin. Mascot was searched using a fragment ion mass tolerance of 0.80 Da, a parent ion tolerance of 1.8 Da, and variable modifications of methionine oxidation. A probability based Mascot score greater than 60 (equivalent to $P \leq 0.05$) was considered a statistically significant hit.

RESULTS

GSH Analysis by HPLC

The overall goal of these studies was to evaluate alterations in thiol to disulfide/oxidized thiol levels in specific proteins after NA or DEM administration. Therefore, initial studies were done to establish doses of these chemicals that produced comparable levels of depletion of soluble thiol (GSH) in airway epithelial cells. Levels of GSH per mg protein in airway epithelial cells of vehicle-treated mice were 37% higher ($P < 0.05$) than in the residual lung of those same animals (Figure 1). As expected, the levels in the airway epithelium and residual lung were less than in the liver. Administration of NA (200 or 300 mg/kg intraperitoneally) or DEM (1 g/kg) resulted in significant loss of GSH in all compartments studied. As a percentage of control, the decrease in GSH levels was greater in airway epithelial cells obtained by lysis lavage than in residual lung, representing a loss to 44% of control in lysis lavage and to 76% of control in residual lung at 200 mg/kg NA. Hepatic GSH levels were depleted to approximately 26% of control at the 200 mg/kg dose. Higher doses of NA decreased GSH levels to less than 15, 44, and 7% of control values in airway epithelium, residual lung, and liver, respectively (Figure 1). DEM treatment (1 g/kg intraperitoneally) resulted in depletion of GSH in airway epithelial cells and liver to levels that were nearly identical to those measured after 300 mg/kg NA administration. The GSH levels in airway epithelial cells after DEM and 300 mg/kg NA treatment were not statistically different from one another. In comparison, NA (300 mg/kg) resulted in depletion of GSH to 44% of control in residual lung compared with 13% of control after DEM; these differences were statistically significant.

Alterations in Protein Thiols in Airway Epithelium after NA or DEM

Proteins were separated by 2D gel electrophoresis within pH ranges of 4.4 to 5.5 and 5.5 to 6.7 (Figures 2A and 2B, respectively). An average of Cy3 fluorescence/Cy5 fluorescence was calculated for each individual spot feature in each treatment group. Of the 906 spot features detected on the pH 4.5 to 5.5 gel images, 190 were identified that differed significantly ($P \leq 0.05$) between the four treatment groups (control, 200 mg/kg NA, 300 mg/kg NA, 1 g/kg DEM; $n = 6$). Of those identified as having significant differences in the ratios of maleimide labeling, 44 could be accurately excised from a control sample separated by 2D gel electrophoresis and stained with silver nitrate. Of those, 13 were identified by MALDI-TOF/TOF analysis, and 33 were identified by LC/MS/MS (with two spots identified by both techniques) after database searches of the MS and MS/MS spectra (Table 1). Of the 234 spot features detected on the pH 5.5 to 6.7 gel images, 51 were identified that had maleimide labeling ratios that differed significantly ($P \leq 0.05$) between the four treatment groups (control, 200 mg/kg NA, 300 mg/kg NA, 1 g/kg DEM; $n = 6$). Of those identified as significant, 11 could be accurately excised and identified from a control sample separated by 2D gel electrophoresis and stained with silver nitrate (Table 1).

One of the primary objectives of these studies was to compare proteins undergoing differential oxidation after cytotoxic

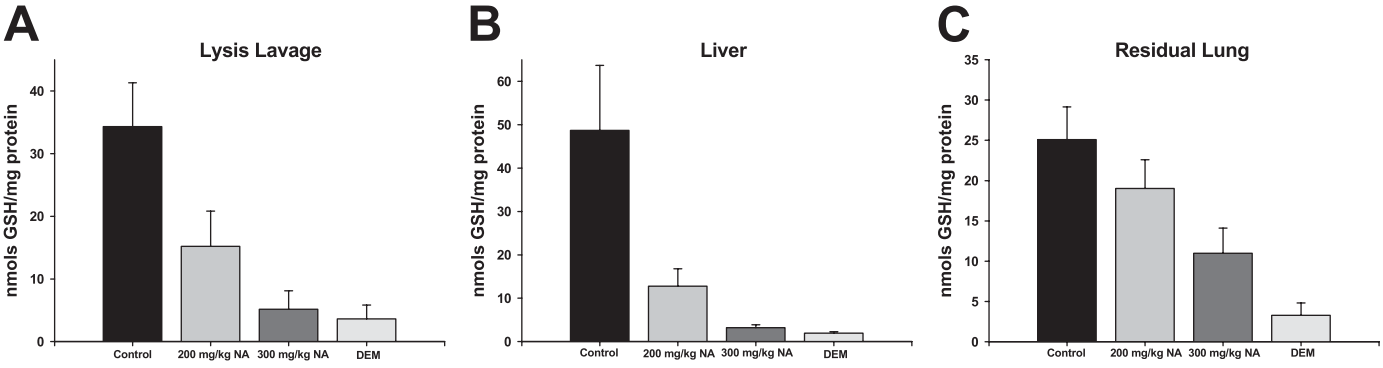

Figure 1. Glutathione levels in lysis lavage, liver, and residual lung samples from mice treated intraperitoneally with vehicle control, 200 mg/kg naphthalene (NA), 300 mg/kg NA or 1 g/kg diethyl maleate (DEM). Animals were killed 2 hours (control, naphthalene) or 1 hour (DEM) after treatment. Values are the mean ± SD ($n = 6$).

TABLE 1. PROTEINS WITH SIGNIFICANT CHANGES IN CY3/CY5 BINDING RATIOS BETWEEN AT LEAST TWO TREATMENT GROUPS IDENTIFIED BY MATRIX-ASSISTED LASER DESORPTION/IONIZATION TANDEM TIME-OF-FLIGHT MASS SPECTROMETRY OR LIQUID CHROMATOGRAPHY–TANDEM MASS SPECTROMETRY

			Statistically Different				Statistically Different											
	Spot #	200 mg/kg NA	Control	300 mg/kg	DEM	300 mg/kg NA	Control	DEM	DEM	Control	Protein Name	Swiss-Prot. Acc. no.	Score	Peptide Count†	% Seq. Cov.	# Cys‡	Mole %§	Ontogeny
pH range 4.5–5.5	1	3.47	—	—	—	2.17	x	—	1.97	—	vinculin	Q64727	2373	71	58	10	0.938	cell adhesion
	2	1.03	—	—	—	0.840	—	—	0.450	x	gelsolin, isoform 2	P13020-2	368	12	22	5	0.684	cytoskeletal
	3	1.11	—	—	—	1.44	—	—	0.389	x	BiP, heat-shock 70-kD protein 5	P20029	1297	38	49	2	0.305	chaperone protein/ protein folding
	4¶	0.885	—	—	—	1.09	—	x	0.262	x	zinc finger protein 354A	Q7M6W9*	63	17	27	46	7.629	transcriptional
	5¶	0.763	—	—	—	1.16	—	—	0.307	x	cysteine and glycine-rich protein 3	P50462	63	9	30	16	8.247	signal transduction
	6	0.714	—	—	—	1.28	—	x	0.459	—	dihydropyrimidinase-like 2	O08553	424	15	31	7	1.224	cytoskeletal
	7	1.02	—	—	—	1.44	—	—	0.398	x	dihydropyrimidinase-like 2	O08553	511	17	41	7	1.224	cytoskeletal
	8	1.15	—	—	—	1.02	—	—	0.431	x	dihydropyrimidinase-like 2	O08553	438	15	35	7	1.224	cytoskeletal
	9	0.562	—	—	—	1.07	—	—	0.268	x	dihydropyrimidinase-like 2	O08553	755	22	50	7	1.224	cytoskeletal
	10¶	1.05	—	—	—	2.25	—	x	0.481	—	surfeit locus protein 6	P70279	68	13	26	2	0.563	
	11	0.595	—	x	—	1.41	—	—	1.15	—	serine/cysteine peptidase inhibitor	Q08EA5*	412	13	27	7	1.703	protease inhibitor
	12¶	0.532	—	x	—	1.14	—	—	1.08	—	zinc finger protein 758	Q8CFF3*	68	18	40	50	9.174	transcriptional
	13	0.725	—	x	—	1.37	—	—	1.68	—	aldehyde dehydrogenase 2	P47738	302	9	27	9	1.734	metabolic enzyme
	14	0.690	—	x	—	1.38	—	—	1.29	—	selenium-binding protein 1	P17563	300	7	15	10	2.119	
	15	0.741	—	x	—	1.83	x	x	0.990	—	aldehyde dehydrogenase 2	P47738	946	16	43	9	1.734	metabolic enzyme
	16	0.595	x	x	—	1.59	—	—	1.07	—	aldehyde dehydrogenase 2	P47738	765	16	39	9	1.734	metabolic enzyme
	17[a]	0.741	x	x	—	2.02	—	—	1.06	—	aldehyde dehydrogenase 2	P47738	74	2	5	9	1.734	metabolic enzyme
	18	1.14	—	—	—	2.19	—	—	0.342	x	aldehyde dehydrogenase 1A1	P24549	709	19	41	11	2.196	metabolic enzyme
	19	1.00	—	—	—	1.23	—	x	0.353	x	aldehyde ehydrogenase 2	P47738	675	20	42	9	1.734	metabolic enzyme
	20	1.03	—	—	—	1.20	—	x	0.283	x	aldehyde dehydrogenase 2	P47738	855	23	46	9	1.734	metabolic enzyme
	21	1.09	—	—	—	1.87	—	—	0.270	x	aldehyde dehydrogenase 2	P47738	681	22	47	9	1.734	metabolic enzyme
	22	0.676	—	x	—	1.50	—	x	0.189	—	aldehyde dehydrogenase 2	P47738	422	13	31	9	1.734	metabolic enzyme
	23	0.592	—	—	—	1.16	—	x	0.685	—	aldehyde dehydrogenase 2	P47738	762	17	38	9	1.734	metabolic enzyme
	24	0.917	—	—	x	1.61	—	x	0.249	x	heterogeneous nuclear ribonucleoprotein H	O35737	180	5	19	5	1.114	transcriptional
	25	0.885	—	—	—	2.26	—	x	0.495	—	Rab GDP dissociation inhibitor β	Q61598-1	114	3	7	9	2.022	cytoskeletal
	26	1.01	—	—	x	2.74	—	x	0.441	x	Ckb creatine kinase B-type	Q04447	233	6	21	5	1.312	energy transduction
	27¶	0.559	—	x	—	1.33	—	x	0.279	—	hypothetical arginine-rich region containing protein	Q3UHS1*	69	9	63	9	7.377	
	28	0.787	—	—	x	1.75	—	—	0.296	—	alpha-enolase	P17182	399	13	39	6	1.382	metabolic enzyme
	29	1.32	—	—	x	3.06	—	—	0.387	—	alpha-enolase	P17182	433	15	44	6	1.382	metabolic enzyme
	30	1.29	—	—	—	2.02	—	x	0.397	—	alpha-enolase	P17182	966	23	53	6	1.382	metabolic enzyme
	31	1.16	—	—	x	1.71	—	—	0.267	—	alpha-enolase	P17182	475	14	37	6	1.382	metabolic enzyme
	32	1.09	—	—	—	2.27	—	x	0.269	—	cytoplasmic gamma actin	Q3TSB7*	1159	20	47	6	1.6	cytoskeletal
	33¶	0.909	—	—	—	2.01	—	x	0.298	—	cytoplasmic beta actin	P60710	258	8	29	6	1.6	cytoskeletal
	34¶	0.549	—	—	—	1.09	—	x	0.242	—	cytoplasmic beta actin	P60710	73	7	28	6	1.6	cytoskeletal
	35	0.332	x	—	—	0.625	—	—	0.500	—	EH domain containing protein 1	Q9WVK4	74	2	13	1	0.187	endosomal transport
	36	0.990	—	—	—	2.62	—	x	0.680	—	annexin A1	P10107	536	21	41	5	1.445	cell growth/signal transduction
	37¶	0.493	—	—	—	1.28	—	x	0.201	—	annexin A3	O35639	66	11	32	3	0.929	cell growth/signal transduction
	38	0.699	—	—	—	1.37	—	x	0.360	—	annexin A3	O35639	780	18	60	3	0.929	cell growth/signal transduction
	39	0.735	—	—	—	1.35	—	x	0.170	—	lactate dehydrogenase B	P16125	246	11	38	5	1.497	metabolic enzyme
	40¶	0.362	x	—	—	0.752	—	—	0.730	—	serine preptidase inhibitor	Q148R4*	73	24	31	61	5.998	protease inhibitor
	41¶	0.415	x	—	—	0.855	—	—	0.775	—	annexin A5	P48036	83	10	31	1	0.313	cell growth/signal transduction
	41	0.415	x	—	—	0.855	—	—	0.775	—	annexin A5	P48036	681	24	62	1	0.313	cell growth/signal transduction
	42¶	0.483	x	—	—	1.44	—	—	0.263	x	regulator of sex-limitation candidate 12	Q7M6W9*	68	18	29	46	7.629	
	43¶	0.952	—	—	—	0.870	—	x	0.168	—	Rho GDP-dissociation inhibitor 1	Q99PT1	188	8	37	1	0.49	cytoskeletal
	43	0.952	—	—	—	0.870	—	x	0.168	—	Rho GDP-dissociation inhibitor 1	Q99PT1	575	15	53	1	0.49	cytoskeletal
	44	1.92	—	—	—	2.76	x	—	1.24	—	peroxiredoxin 1	P35700	250	9	44	4	2.01	redox protein

(*continued*)

TABLE 1. (CONTINUED)

	Spot #	200 mg/kg NA	Statistically Different: Control	300 mg/kg	DEM	300 mg/kg NA	Statistically Different: Control	DEM	DEM	Control	Protein Name	Swiss-Prot. Acc. no.	Score	Peptide Count†	% Seq. Cov.	# Cys‡	Mole %§	Ontogeny
pH range 5.5–6.7	1	2.42	—	—	—	5.86	—	—	3.01	x	membrane-organizing extension spike protein	P26041	115	7	13	2	0.347	cytoskeletal
	2	2.35	x	—	—	2.54	—	—	2.37	—	membrane-organizing extension spike protein	P26041	77	4	7	2	0.347	cytoskeletal
	3	1.52	—	—	—	2.72	x	—	1.53	—	isoform 1 of keratin, type 1 cytoskeletal 10	P02535-1	210	7	11	3	0.526	cytoskeletal
	4	2.13	—	—	—	1.26	—	x	2.20	x	keratin, type II cytoskeletal 75	Q8BGZ7	117	2	4	4	0.726	cytoskeletal
	5¶	1.70	—	—	—	2.03	—	—	2.21	x	aldehyde dehydrogenase 1A1	P24549	105	12	27	11	2.196	metabolic enzyme
	6	1.44	—	—	—	3.75	—	—	2.21	x	carboxylesterase 3	Q8VCT4	101	2	3	5	0.885	metabolic enzyme
	7	1.73	—	—	—	4.54	—	—	2.46	x	carboxylesterase 6	Q3TMR2*	176	5	10	8	1.434	metabolic enzyme
	8	0.885	—	—	x	3.00	—	—	1.40	x	heat-shock 70-kDa protein 8	P63017	279	10	16	4	0.619	chaperone protein/ protein folding
	9	2.60	—	—	—	3.43	—	—	3.37	x	GAPDH	P16858	74	3	9	5	1.502	metabolic enzyme
	10	2.14	—	—	—	2.19	x	—	1.88	—	BiP, heat-shock 70-kD protein 5	P20029	95	2	4	2	0.305	chaperone protein/ protein folding
	11	0.775	—	x	—	2.15	x	—	1.61	—	carbonyl reductase 2	P08074	337	12	38	2	0.82	metabolic enzyme

Definition of abbreviations: DEM = diethyl maleate; EH = Eps15 homology.

* A TrEMBL accession number.

† The number of peptides used for database matching.

‡ The number of cysteines present on the protein according to the International Protein Index.

§ The molar percentage of the cysteines in the protein according to the International Protein Index.

¶ The protein was identified by MALDI-TOF/TOF.

doses of NA with nontoxic DEM. Using doses of these two compounds, which produced similar levels of GSH depletion in liver and airway epithelial cells, 16 unique proteins were identified where the Cy3/Cy5 labeling differed significantly. In most cases, this resulted from ratios of Cy3 (reduced)/Cy5 (oxidized and reducible by tributylphosphine) after 300 mg/kg NA, which stayed similar to control values or increased slightly, and decreased dramatically after DEM treatment, in some cases by as much as 5- to 6-fold (Table 1). All but one of the identified proteins demonstrating these differences in the Cy3/Cy5 ratio were observed in the 4.5 to 5.5 pH range. These proteins included metabolic enzymes (aldehyde dehydrogenase, α enolase), structural proteins such as β-actin, and proteins associated with the unfolded protein response (Bip, heat shock 70 kD, protein 5). Mitochondrial aldehyde dehydrogenase, Rho-GDP disassociation inhibitor α, two forms of annexin, and two zinc finger proteins were also identified, among others. For β-actin (spot features #33 and #34), mitochondrial aldehyde dehydrogenase and Bip, the difference in the Cy binding ratio after 300 mg/kg NA results from an increase in Cy3 binding and a decrease in Cy5 binding (Figure 3). In contrast, DEM treatment decreases Cy3 labeling and increases Cy5 labeling of β-actin and mitochondrial aldehyde dehydrogenase; for Bip, Cy3 labeling decreased significantly from control, whereas Cy5 labeling decreased only slightly from control.

Significant changes in Cy3/Cy5 labeling were noted in 10 proteins when comparing the group treated with 200 mg/kg NA with the group treated with 300 mg/kg NA. These proteins included several mitochondrial aldehyde dehydrogenases (Figure 4), serine/cysteine peptidase inhibitor, a zinc finger protein, and selenium binding protein 1. In all cases, 200 mg/kg NA produced a slight decrease in the Cy3/Cy5 ratio, whereas 300 mg/kg NA dose produced an increase in this ratio.

At a dose of 200 mg/kg NA, GSH is depleted to 45% of control in target airway epithelium (*see* Figure 1). This treatment results in a significant decrease in Cy3/Cy5 ratio for five identified proteins when compared with control. These proteins include mitochondrial aldehyde dehydrogenase, serine protease inhibitor, and annexin A5. The differences in the Cy3/Cy5 labeling ratios for all five of the proteins come from a drastic decrease (4-fold less) in the Cy3 labeling in the 200 mg/kg–treated group. A dose of 300 mg/kg NA caused a significant increase in the Cy3/Cy5 labeling ratios of six proteins (vinculin, mitochondrial aldehyde dehydrogenase, peroxiredoxin 1, cytoskeletal keratin, Bip, and carbonyl reductase 2) in comparison to control. The difference in Cy3/Cy5 labeling for these six proteins arises from an increase in Cy3 labeling and a decrease in Cy5 labeling.

DISCUSSION

There has been a long-standing interest in the redox status of soluble and protein sulfhydryls. Recent progress aimed at understanding the response of cells to strongly oxidizing environments has provided important insights into intracellular events that arise in response to exposure to oxidizing chemicals and to diseases that result in higher-than-normal formation of reactive oxygen species. Until recently, our appreciation of the absolute quantities of available protein sulfyhydryl, protein disulfides (PSSP), and protein mixed disulfides with GSH (PSSG) has been limited. Newly introduced approaches for measuring the proportions of protein sulfyhydryl, PSSP, and PSSG in cell lines (HEK and HeLa) show a relatively small number of protein cysteines in disulfide bonds ($< 10\%$) and a small percentage of these as PSSG ($< 0.1\%$), indicating that this is likely not a major source of GSH storage (20). Although these studies provide a reasonable accounting of the proportions of thiols, disulfides, and protein-GSH mixed disulfides, they are not capable of examining the sulfhydryl status of individual proteins. The differential labeling methods introduced earlier (16) are not able to assess the absolute proportions of protein thiols and disulfides in the cell, but they allow evaluation of changes in the oxidation status of cysteines of individual proteins in response to external stimuli.

This study was based on earlier work showing that GSH depletion is a necessary but not sufficient event in NA-induced airway epithelial cell toxicity in mice. Doses of NA that produce substantial depletion of GSH result in necrosis of nonciliated bronchiolar epithelial cells of mouse lung (1, 8, 9). In contrast, at doses that result in comparable levels of GSH depletion, DEM produces transient alterations in Clara cell morphology, including swelling, blebbing, and cytoskeletal disruption, which resolves and does not proceed to frank cellular necrosis (9). The

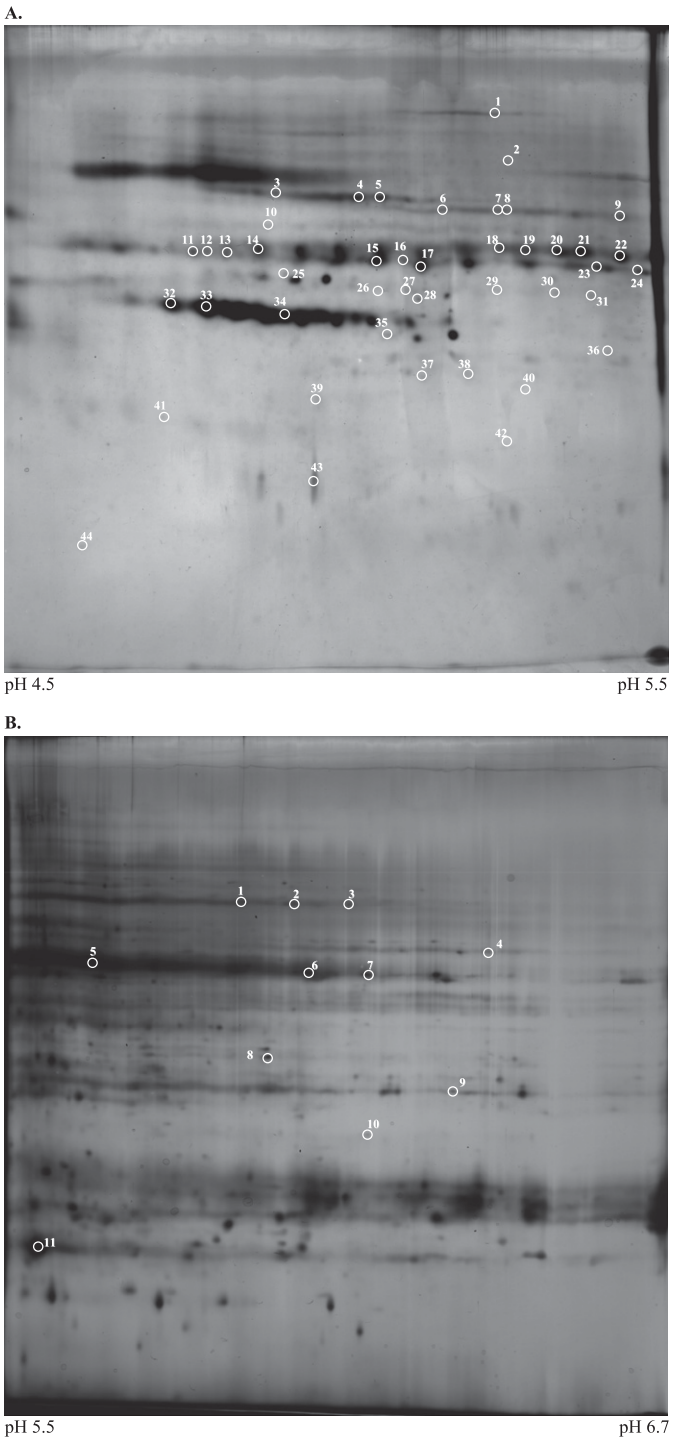

Figure 2. Silver stained gel image of 100 μg of Cy3/Cy5 labeled protein obtained by lysis lavage from control mice separated in (*A*) pH range 4.5 to 5.5 or (*B*) pH range 5.5 to 6.7, depicting the location of (*A*) 44 or (*B*) 11 proteins identified by MALDI-TOF/TOF or LC/MS/MS.

current work has shown that Cy3/Cy5 labeling ratios of a total of 241 separate spot features over a 2 pH range were significantly different among at least two of the treatment groups (control, 200 mg/kg, 300 mg/kg, and 1 g/kg DEM). Of these, 16 proteins isolated from mouse airway epithelial cells from the 300 mg/kg treatment group differed significantly in Cy3/Cy5 labeling ratios, compared with the DEM treatment group.

Different doses and time points for exposure of DEM and NA were used to demonstrate comparable, significant losses in airway epithelial cell GSH levels. GSH levels in the lysis lavage, residual lung, and liver samples (*see* Figure 1) show 200 and 300 mg/kg NA, and DEM treatments depleted GSH levels significantly from control. The fact that NA requires metabolism by cytochrome P450 monooxygenases to produce GSH-depleting metabolites is consistent with the selectivity observed in GSH loss from airway epithelial cells obtained by lysis lavage compared with residual lung. DEM depletes GSH in airway epithelium and residual lung compartments to levels that are comparable to each other, a finding that is consistent with mechanisms of GSH depletion from this chemical that involve GSH transferase-dependent conjugation. The cytochrome P450 monooxygenase that catalyzes the metabolic activation of NA is almost exclusively localized in Clara cells of the airway epithelium (21), whereas GSH transferases are present in airway and alveolar epithelium (22). In lysis lavage and liver samples, 300 mg/kg NA and 1 g/kg DEM treatments depleted GSH to levels that were not statistically different.

Many of the proteins whose thiol status was shown in these studies to be influenced by NA, DEM, or both compounds have been shown to be targets of various electrophilic metabolites derived from hepatic, pulmonary, and renal toxicants. A comprehensive database of adducted proteins is being developed by Hanzlik and colleagues (23; http://tpdb.medchem.ku.edu:8080/protein_database/). Even though this list is incomplete, proteins such as BiP, heat-shock protein 70, selenium binding protein, aldehyde dehydrogenase, and β- and γ-actin are common targets for a number of reactive metabolites generated by cytochrome P450–dependent metabolism. Although there is no conclusive evidence for the formation of one or more specific adduct(s) in cytotoxicity, the availability of a more complete database of cellular proteins being modified by these reactive metabolites has enabled testable hypothesis to be formulated. As discussed in detail by Ikehata and colleagues (24), many of the targeted proteins for reactive metabolites are associated with chaperones, and adduction of these proteins is consistent with the possibility that they are important in the series of events that lead to cytotoxicity. GSH depletion is one of the hallmark events associated with many of these toxicants. GSH depletion exposes the cell to additional stress associated with loss of one of the main cellular protection systems, which in turn generates unfolded proteins, placing additional demands on the chaperone proteins. Although this explanation is appropriate for an acute exposure, as seen in this 2-hour study, different cellular mechanisms, such as an increase in *de novo* protein synthesis, may play significant roles over longer periods of time where an increase in oxidative stress is known to result in increased transcription of antioxidant genes, including those of chaperone proteins. Support for this comes from recent studies in lungs of smokers compared with nonsmokers that demonstrate significantly higher levels of several endoplasmic reticulum stress proteins (calreticulin, protein disulfide isomerase, and GRP 78) in smokers (25). These same proteins have been identified in studies from our lab as targets for reactive NA or nitronaphthalene metabolites (13, 14, 26) or with thiol ratios that are significantly altered by NA or DEM treatment in this study. As demonstrated in the current work, DEM treatment decreased the Cy3/Cy5 ratios for two heat-shock proteins (BiP and Hspa8; 70 kD) in comparison to control. This latter protein is adducted by reactive NA metabolites in airway epithelial cells (13), which may alter its ability to act as a chaperone.

In numerous cases, statistically significant differences in thiol labeling ratios between 300 mg/kg NA and DEM resulted from slightly higher Cy3/Cy5 ratios after NA compared with control

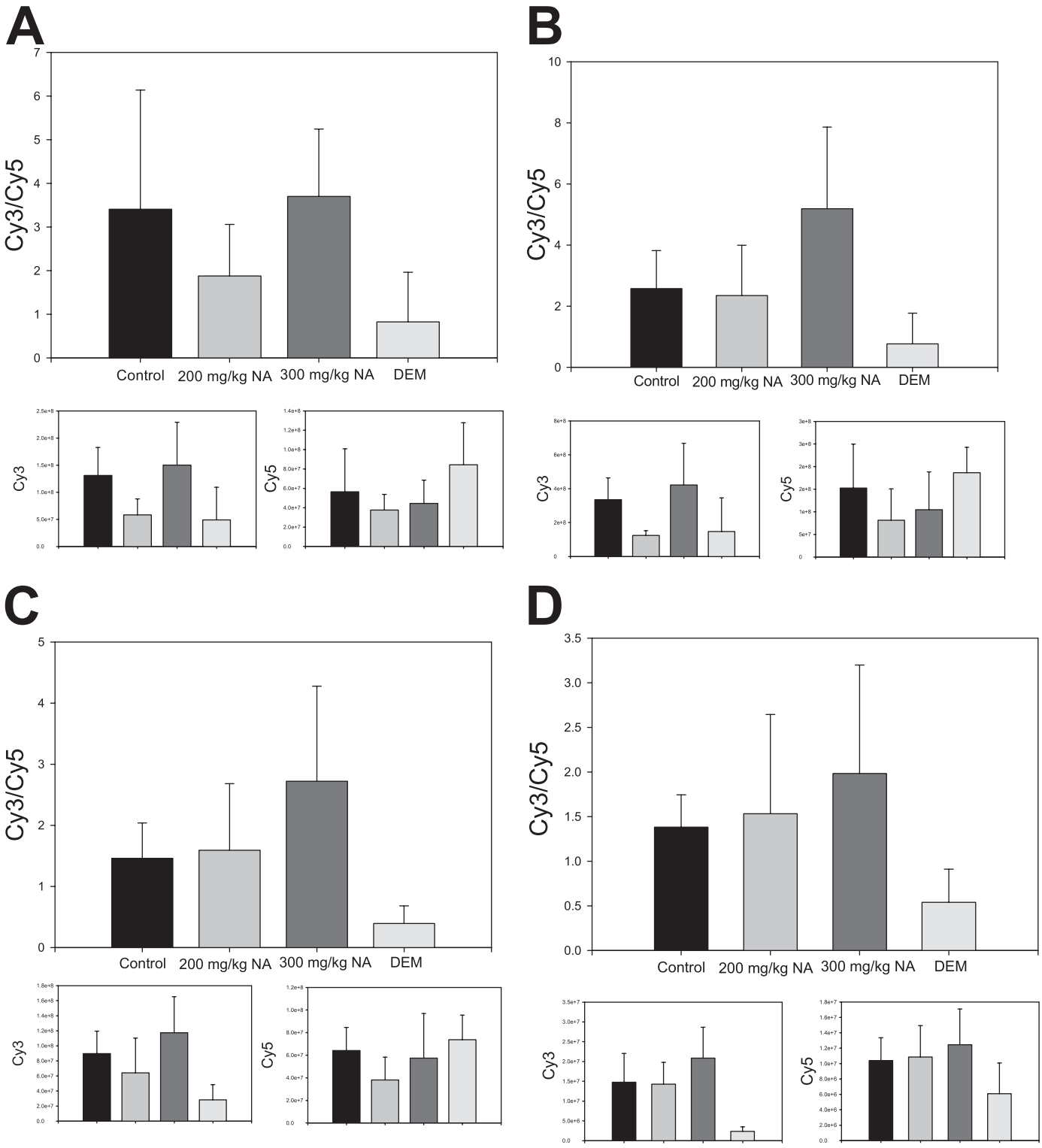

Figure 3. Cy3/Cy5 labeling ratios for representative proteins showing significant differences in labeling ratios for NA (300 mg/kg) compared with DEM treatment. The *bar graphs* show labeling intensity of Cy3/Cy5 ratios along with Cy3 and Cy5 values for β-actin (*A*: spot #33), β-actin (*B*: spot #34), mitochondrial aldehyde dehydrogenase (*C*: spot #21), and Bip (*D*: spot #3). Values are the mean ± SD ($n = 3$).

and decreased Cy3/Cy5 labeling with DEM compared with control. For example, with β-actin, a highly abundant protein, the increase in Cy3/Cy5 was due to a loss of Cy5 signal and a gain in Cy3 labeling after NA treatment. One possible explanation of these findings that is consistent with the increase in Cy3 labeling involves deglutathionylation of the protein from its native state, possibly brought on by the oxidative stress in the airway epithelial cells. Actin is constitutively glutathionylated in cells even in the absence of oxidative stress (27, 28). Glutathionylation inhibits actin polymerization *in vitro* and affects the cellular cytoskeleton (27–29). One of the earliest events of NA-induced Clara cell cytotoxicity is cytoskeletal rearrange-

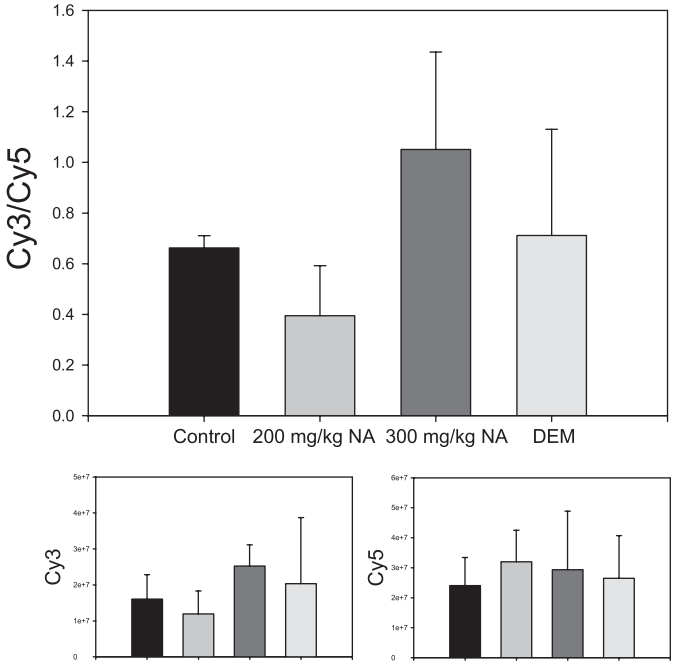

Figure 4. Cy3/Cy5 labeling ratios for a mitochondrial aldehyde dehydrogenase protein, showing significant differences in labeling ratios for 200 mg/kg NA compared with 300 mg/kg NA. The *bar graphs* show labeling intensity of Cy3/Cy5 ratios along with Cy3 and Cy5 values for mitochondrial aldehyde dehydrogenase (spot #16). Values are the mean ± SD ($n = 3$).

ment within swollen cells, where filaments relocate to the apex of the cell and apical membrane blebs are separated from the main body of the cell by a zone of organized filaments (30). The filaments caused by NA cytotoxicity are present 2 hours after treatment and organize into blebs at 3 hours after treatment (30). The Clara cell blebs resemble those found in hepatocytes exposed *in vitro* and *in vivo* to decarbazine and menadione, a compound known to redox cycle, thereby generating reactive oxygen species (31–33).

Another protein found to have a significant change in its Cy3/Cy5 binding ratio in the 300 mg/kg treatment group was a Rho guanine-nucleotide-dissociation inhibitor α (RHO-GDIα). Rho-GDIs stabilize the GDP-bound inactive state of small G proteins known as GTPases *in vitro* and *in vivo* (34–38). GTPases regulate cell functions such as growth and differentiation, as well as cytoskeletal architecture and other cell functions (39–43). In GDI-negative cells, protrusions and actin-rich structures were found at the cell periphery and were shown to be driven by actin polymerization (44).

The primary purpose of the studies reported here was to compare changes in the status of protein sulfhydryls in response to GSH depletion with one of the chemicals producing dose-dependent necrosis of airway Clara cells (NA) and the other producing some signs of cellular stress that resolves without lethal injury (DEM). The doses used in these studies are well above those to which humans are exposed. Although the primary route of human exposure is via inhalation, toxicant was administered intraperitoneally to allow consistent control of the dosing regimen. Comparison of the Clara cell injury in proximal airways after inhalation and intraperitoneal doses indicates that exposure to very low concentrations (2–5 ppm) yields cytotoxicity equivalent to approximately 50 to 100 mg/kg intraperitoneally, whereas exposure to higher concentrations (10 ppm) yields results approximately equivalent to 200 mg/kg doses (2). Although 10-ppm levels are well above those normally found in ambient atmospheres, the long-term, consistent nature of human exposure (compared with the acute studies that comprise the bulk of the available data on NA) raises concerns about the long-term health effects of this and similar chemicals.

The findings in this study have not been independently confirmed with alternate methodology. However, the initial studies (16), done to develop and verify the approaches used here, carefully optimized reagent concentrations to obtain complete derivatization of available protein sulfhydryls and reduction of disulfides. Experiments with purified proteins with varying thiol:disulfide ratios yielded the expected results over a range of protein concentrations. Other groups have used similar approaches involving the use of maleimide dyes in the near-infrared range (45) and the DIGE dyes prepared for saturation labeling (46, 47). The dyes used in the current work are the disulfonic acid maleimides, which have better water solubility than the charge-matched, saturation labeling dyes, but they cause a shift in the apparent pH of the proteins to the acididic range, resulting in a higher number of spots in the 4.5 to 5.5 range than in the 5.5 to 6.7 range. In direct comparisons between ICAT labeling and DIGE maleimide dye labeling, Fu and colleagues (46) identified a total of 50 proteins that were posttranslationally modified by H_2O_2. Only 13 of these were identified by both methods. LC/MS/MS methods focus on measurement of tryptic peptides and as a result tend to work better than gel electrophoresis for high-molecular-weight and membrane-bound proteins. In addition, the authors used broad range IPG strips for their electrophoresis, and there is a significant possibility that low-abundance proteins could not be detected. The methods used in the current studies relied on narrow-range IPG strips to provide better protein resolution and higher loading capacities. Moreover, the use of disulfonic acid dyes increases the solubility of the derivatives, allowing higher protein gel loading. Nevertheless, we recognize the possibility that proteins imaged on our gels could contain more than one protein, thus leading to false-negative results in cases where the ratios of reduced to oxidized thiols of a lower abundance protein have been modified significantly by NA or DEM but were not detected because of signal from a protein registered at the same location of the gel that was not altered.

In conclusion, these studies suggest that moderate and high doses of NA cause significant changes in the protein thiol status of specific proteins. It is unclear whether alterations in the thiol state of these proteins alter their function within the airway epithelial cells. Noncytotoxic DEM causes significant and often drastically different changes in protein thiols identified by this study. Results from this study, combined with previous work from our laboratory and that of others, indicate there are specific proteins and protein families that are targeted for adduction and oxidation by reactive NA metabolites. Identified proteins are not always the most abundant within airway epithelial cells, nor do they all contain a large percentage of cysteines. Thus, target proteins may contain very reactive thiols that react selectively with oxidants generated during NA metabolism. This is a significant but preliminary step in determining which proteins are disrupted by NA that leads to cellular stress and necrosis in the rodent pulmonary epithelial cell. Additional studies are underway to compare protein thiol loss in airway epithelium in response to NA metabolites (NA, 1,2-NA oxide, and 1,2- and 1,4-naphthoquinone) because a clearer understanding of the metabolites associated with toxicity is important to understanding the potential interindividual differences in susceptibility that may be associated with NA exposure.

Author Disclosure: P.S. received $10,001 to $50,000 from NIEHS for a Predoctoral Training Fellowship (ES007059-30). A.B. received consultancy fees from Health Effects Institute for <$1,000 along with lecture fees from American Petroleum Institute for less than $1,000 for a presentation at the annual conference and a grant for $10,000 to $50,000. His spouse/life partner owns stock in ExxonMobil for more than $100,001, and he received a sponsored grant from NIH for more than $100,001 for grants R01/P42. He also received less than $1,000 from Phillip Morris for reviewing two grants 8 years ago and received a stipend (~$100 each). D.M. received a sponsored grant from NIEHS for $50,001 to $100,000. None of the other authors has a financial relationship with a commercial entity that has an interest in the subject of this manuscript.

Acknowledgments: The authors thank the University of California, Davis, Proteomics Facility for analyzing a portion of the protein samples presented herein.

References

1. Plopper CG, Suverkropp C, Morin D, Nishio S, Buckpitt A. Relationship of cytochrome P-450 activity to Clara cell cytotoxicity: I. Histopathologic comparison of the respiratory tract of mice, rats and hamsters after parenteral administration of naphthalene. *J Pharmacol Exp Ther* 1992;261:353–363.
2. West JAA, Pakehham G, Morin D, Fleschner CA, Buckpitt AR, Plopper CG. Inhaled naphthalene causes dose dependent Clara cell cytotoxicity in mice but not in rats. *Toxicol Appl Pharmacol* 2001;173:114–119.
3. ATSDR. Toxicological profile for naphthalene: toxicological profile for naphthalene, 1-methylnaphthalene, and 2-ethylnaphthalene. Washington, DC: US Department of Health and Human Services; 2005.
4. Witschi H, Espiritu I, Maronpot RR, Pinkerton KE, Jones AD. The carcinogenic potential of the gas phase of environmental tobacco smoke. *Carcinogenesis* 1997;8:2035–2042.
5. Kobayashi R, Okamoto RA, Maddalena RL, Kado NY. Polycyclic aromatic hydrocarbons in edible grain: a pilot study of agricultural crops as a human exposure pathway for environmental contaminants using wheat as a model crop. *Environ Res* 2008;107:145–151.
6. Li Z, Sandau CD, Romanoff LC, Caudill SP, Sjodin A, Needham LL, Patterson DG Jr. Concentration and profile of 22 urinary poly aromatic hydrocarbon metabolites in the US population. *Environ Res* 2008;107:320–331.
7. Warren DL, Brown DL Jr, Buckpitt AR. Evidence for cytochrome P-450 mediated metabolism in the bronchiolar damage by naphthalene. *Chem Biol Interact* 1982;40:287–303.
8. Phimister AJ, Lee MG, Morin D, Buckpitt AR, Plopper CG. Glutathione depletion is a major determinant of inhaled naphthalene respiratory toxicity and naphthalene metabolism in mice. *Toxicol Sci* 2004;82:268–278.
9. Phimister AJ, Williams KJ, Van Winkle LS, Plopper CG. Consequences of abrupt glutathione depletion in murine Clara cells: ultrastructural and biochemical investigations into the role of glutathione loss in naphthalene cytotoxicity. *J Pharmacol Exp Ther* 2005;314:506–513.
10. Cho M, Chichester C, Morin D, Plopper C, Buckpitt A. Covalent interactions of reactive naphthalene metabolites with proteins. *J Pharmacol Exp Ther* 1994;269:881–889.
11. Zheng J, Cho M, Jones AD, Hammock BD. Evidence of quinone metabolites of naphthalene covalently bound to sulfur nucleophiles of proteins of murine Clara cells after exposure to naphthalene. *Chem Res Toxicol* 1997;10:1008–1014.
12. Isbell MA, Morin D, Boland BC, Buckpitt AR, Salemi MR, Presley J. Identification of proteins adducted by reactive naphthalene metabolites *in vitro*. *Proteomics* 2005;5:4197–4204.
13. Lin CY, Isbell MA, Morin D, Boland BC, Salemi MR, Jewell WT, Weir AJ, Fanucchi MV, Baker GL, Plopper CG, *et al.* Characterization of a structurally intact in situ lung model and comparison of naphthalene protein adducts generated in this model vs lung microsomes. *Chem Res Toxicol* 2005;18:802–813.
14. Lin CY, Boland BC, Jin Lee Y, Salemi MR, Morin D, Miller LA, Plopper CG, Buckpitt AR. Identification of proteins adducted by reactive metabolites of naphthalene and 1-nitronaphthalene in dissected airways of rhesus macaques. *Proteomics* 2006;6:962–982.
15. Dennehy MK, Richards KAM, Wernke GR, Shyr Y, Liebler DC. Cytosolic and nuclear protein targets of thiol-reactive electrophiles. *Chem Res Toxicol* 2006;19:20–29.
16. Spiess PC, Morin D, Jewell WT, Buckpitt AR. Measurement of protein sulfhydryls in response to cellular oxidative stress using gel electrophoresis and multiplexed fluorescent imaging analysis. *Chem Res Toxicol* 2008;21:1074–1085.
17. Wheelock AM, Zhang L, Tran M-U, Morin D, Penn S, Buckpitt AR, Plopper CG. Isolation of rodent airway epithelial cell proteins facilitates in vivo proteomics studies of lung toxicity. *Am J Physiol Lung Cell Mol Physiol* 2004;286:L399–L410.
18. Lakritz J, Plopper CG, Buckpitt AR. Validated high-performance liquid chromatography-electrochemical method for determination of glutathione and glutathione disulfide in small tissue samples. *Anal Biochem* 1997;247:63–68.
19. Bradford MM. A rapid and sensitive method for the quantification of microgram quantities of protein utilizing the principle of protein-dye binding. *Anal Biochem* 1976;72:248–254.
20. Hansen RE, Roth D, Winther JR. Quantifying the global cellular thiol-disulfide status. *Proc Natl Acad Sci USA* 2009;106:422–427.
21. Buckpitt A, Chang AM, Weir A, Van Winkle L, Duan X, Philpot R, Plopper C. Relationship of cytochrome P450 activity to Clara cell cytotoxicity: IV. Metabolism of naphthalene and naphthalene oxide in microdissected airways from mice, rats, and hamsters. *Mol Pharmacol* 1995;47:74–81.
22. Forkert PG, D'Costa D, El Mestrah M. Expression and inducibility of alpha, pi, and Mu glutathione S-transferase protein and mRNA in murine lung. *Am J Respir Cell Mol Biol* 1999;20:143–152.
23. Hanzlik RP, Koen YM, Theertham B, Dong Y, Fang J. The reactive metabolite target protein database (TPDB): a web-accessible resource. *BMC Bioinformatics* 2007;8:95.
24. Ikehata OK, Duzhak TG, Galeva NA, Ji T, Koen YM, Hanzlik RP. Protein targets of reactive metabolites of thiobenzamide in rat liver in vivo. *Chem Res Toxicol* 2008;21:1432–1442.
25. Kelsen S, Duan X, Ji R, Perez O, Liu C, Merali S. Cigarette smoke induces an unfolded protein response in the human lung: a proteomic approach. *Am J Respir Cell Mol Biol* 2008;38:541–550.
26. Wheelock AM, Boland BC, Isbell M, Morin D, Wegesser TC, Plopper CG, Buckpitt AR. In vivo effects of ozone exposure on protein adduct formation by 1-nitronaphthalene in rat lung. *Am J Respir Cell Mol Biol* 2005;33:130–137.
27. Wang J, Boja ES, Tan W, Tekle E, Fales HM, English S, Mieyal JJ, Chock PB. Reversible glutathionylation regulates actin polymerization in A431 cells. *J Biol Chem* 2001;276:47763–47766.
28. Wang J, Tekle E, Oubrahim H, Mieyal JJ, Stadtman ER, Chock PB. RNA interference: investigating the physiological function of glutathionylated actin. *Proc Natl Acad Sci USA* 2003;100:5103–5106.
29. Dalle-Donne I, Giustarini D, Rossi R, Colombo R, Milzani A. Reversible S-glutathionlyation of cys374 regulated actin filament formation by inducing structural changes in the actin molecule. *Free Radic Biol Med* 2003;34:23–32.
30. Van Winkle LS, Johnson ZA, Nishio SJ, Brown CD, Plopper CG. Early events in naphthalene-induced acute Clara cell toxicity: comparison of membrane permeability and ultrastructure. *Am J Respir Cell Mol Biol* 1999;21:44–53.
31. Dancygier H, Runne U, Leuschner U, Milbradt R, Classen M. Decabazine (DTIC)-induced human liver damage light and electron-microscopic findings. *Hepatogastroenterology* 1983;30:93–95.
32. Malorni W, Iosi F, Mirabelli F, Bellomo G. Cytoskeleton as a target in menadione-induced oxidative stress in cultured mammalian cells: alterations underlying surface bleb formation. *Chem Biol Interact* 1991;80:217–236.
33. Mirabelli F, Salis A, Marinoni V, Finardi G, Bellomo G, Thor H, Orrenius S. Menadione-induced bleb formation in hepatocytes as associated with the oxidation of thiol groups in actin. *Arch Biochem Biophys* 1988;264:261–269.
34. Kuroda S, Kikuchi A, Hirata K, Masuda T, Kishi K, Sasaki T, Takai Y. Cooperative function of *rho* GDS and *rho* GDI to regulate *rho* p21 activation in smooth muscle. *Biochem Biophys Res Commun* 1992;185:473–480.
35. Bourmeyster N, Boquet P, Vignais PV. Role of bound GDP in the stability of the Rho A-Rho GDI complex purified from neutrophil cytosol. *Biochem Biophys Res Commun* 1994;205:174–179.
36. Wu WJ, Leonard DA, Cerione R, Manor D. Interaction between Cdc42Hs and RhoGDI is mediated through the Rho insert region. *J Biol Chem* 1997;272:26153–26158.
37. Leonard D, Hart MJ, Platko JV, Eva A, Henzel W, Evans T, Cerione RA. The identification and characterization of a GDP-dissociation inhibitor (GDI) for the CDC42Hs protein. *J Biol Chem* 1992;267:22860–22868.
38. Kikuchi A, Kuroda S, Sasaki T, Kotani K, Hirata K, Katayama M, Takai Y. Functional interactions of stimulatory and inhibitory GDP/GTP exchange proteins and their common substrate small GTP-binding protein. *J Biol Chem* 1992;267:14611–14615.

39. Boguski M, McCormick F. Proteins regulating Ras and its relatives. *Nature* 1993;366:643–654.
40. Nobes C, Hall A. Rho, Rac, and Cdc42 GTPases regulate the assembly of multimolecular focal complexes associated with actin stress fibers, lamellipodia, and filopodia. *Cell* 1995;81:53–62.
41. Ridley A, Hall A. The small GTP-binding protein rho regulates the assembly of focal adhesions and actin stress fibers in response to growth factors. *Cell* 1992;70:389–399.
42. Michiels F, Habets GGM. A role for Rac in Tiam1-induced membrane ruffling and invasion. *Nature* 1995;375:338–340.
43. Stowers L, Yelon D, Berg LJ, Chant J. Regulation of the polarization of T cells toward antigen-presenting cells by Ras-related GTPase CDC42. *Proc Natl Acad Sci USA* 1995;92:5027–5031.
44. Rivero F, Illenberger D, Somesh BP, Dislich H, Adam N, Meyer AK. Defects in cytokinesis, actin reorganization and the contractile vacuole in cells deficient in RhoGDI. *Euro Molec Biol Org J* 2002;21: 4539–4549.
45. Riederer IM, Herrero RM, Leuba G, Riederer BM. Serial protein labeling with infrared maleimide dyes to identify cysteine modifications. *J Proteomics* 2008;71:222–230.
46. Fu C, Hu J, Liu T, Ago T, Sadoshima J, Li H. Quantitative analysis of redox-sensitive proteome with DIGE and ICAT. *J Proteome Res* 2008;7:3789–3802.
47. Hurd TR, James AM, Lilley KS, Murphy MP. Measuring redox changes to mitochondrial protein thiols with redox difference gel electrophoresis (redox-DIGE). *Methods Enzymol* 2009;456:343–361.